Mid-infrared absorption of trapped electrons in titanium(IV) oxide particles using a photoacoustic FTIR technique

Mid-infrared absorption of trapped electrons in titanium(IV) oxide particles using a photoacoustic FTIR technique

Naoya Murakami*[a,b] and Tatsuki Shinoda [b]

[a]Department of Applied Chemistry, Faculty of Engineering, Kyushu Institute of Technology, 1-1 Sensuicho, Tobata, Kitakyushu 804-8550, Japan.

[b]Graduate School of Life Science and Systems Engineering, Kyushu Institute of Technology, 2-4 Hibikino, Wakamatsu-ku, Kitakyushu 808-0196, Japan.

Mid-infrared absorption of titanium(IV) oxide (TiO_2) under ultraviolet (UV) irradiation was studied by Fourier transform infrared spectroscopy using a photoacoustic (PA) technique. UV irradiation induced an upward shift of PA spectra, which is due to trivalent titanium (Ti^{3+}) species produced by electron accumulation. The PA spectra under UV irradiation mainly depend on the crystal structure, indicating that energy levels of Ti^{3+} is largely determined by crystal structures.

Photocatalytic reactions over semiconductor materials using above-band gap excitation are induced by photoexcited electrons and positive holes, and the photoexcited electrons and positive holes migrate in the bulk and react with adsorbates on the surface. However, some of them are stabilized at trapping states or undergo recombination with each other at deeper states, which are called recombination centres. Thus, these localized electronic states are important factors that determine the rate of a photocatalytic reaction in addition to the generally considered properties, such as specific surface area, particle size, and crystal structure. The impact of these states on photocatalytic properties has been pointed out, and these states are attributed to crystal defects and impurities in a semiconductor.[1]

A possible structure of defects in titanium(IV) oxide (TiO_2), which is a representative semiconductor photocatalyst used in practical application,[2–6] is trivalent titanium (Ti^{3+}) species, and it forms by electron trapping at a five-coordinate titanium ion with an oxygen vacancy. An almost linear relation between Ti^{3+} density and recombination rate constant among several TiO_2 samples[7] indicates that Ti^{3+} density is an empirical value of the defect density in TiO_2. Therefore, Ti^{3+} species in TiO_2 particles have been studied by a photochemical method using methyl viologen[7], electron spin resonance[7–11], and electronic absorption spectroscopy[12,13]. However, there are few studies on the energy levels of Ti^{3+} in TiO_2 particles, though the probability of trapping and recombination is considered to be determined also by the energy level.

Some studies have shown that energy levels of an electron trapping site lie 0–0.4 eV below the bottom of the conduction band in TiO_2,[7, 14,15] and excitation energy from the trapping site to the bottom of the conduction band corresponds to photon energy of the mid-infrared region (< ca. 3200 cm^{-1}). Thus, Fourier transform infrared spectroscopy (FTIR) can be used for analysis of the energy levels of Ti^{3+} in TiO_2 particles. Actually, a number of FTIR studies have been carried out for detecting photogenerated Ti^{3+} species.[16–27] However, a special set-up has often been needed to estimate photoabsorption of semiconductor particles

because accurate evaluation is difficult for strongly scattering materials and water-adsorbed materials, such as TiO_2 particles. As a result, most of the measurements require special pretreatments and/or conditions, such as high vacuum or low temperature, which is far from the ordinary conditions for photocatalytic reactions. Moreover, the pretreatments and conditions may change the properties of sample particles.

Recently, the attenuated total reflection (ATR) technique has been widely used for FTIR measurements to observe a catalytic interface during illumination.[18,21,24−27] The ATR technique is suitable for investigating solid–liquid interfaces of particles. However, particle size must be below the penetration depth of light in order to obtain information on the gas phase over a catalyst because the sample is photoirradiated from the opposite side to the solid–liquid interface that is observed by the ATR technique. Therefore, systematic measurements of TiO_2 particles with various sizes by the ATR method is difficult.

A photoacoustic (PA) technique can be used for in situ observation of Ti^{3+} under a photocatalytic condition without any pretreatment, and it is applicable to even opaque and strongly scattering solid materials because photoabsorption is detected by photothermal waves.[28,29] In the previous study, we established a photoacoustic Fourier transform infrared spectroscopy (FTIR-PAS) system for in situ observation of a photocatalytic reaction over TiO_2 particles.[30] In the present study, the FTIR-PAS system was extended to a system for analysis of the energy level of Ti^{3+} by detecting low photon energy absorption (0.1−0.7 eV). Moreover, it was applied to various kinds of TiO_2 particles with different crystal structures. As far as we know, this is the first report on analysis of crystal structure dependence.

Detailed setups for FTIR-PAS measurements were reported previously.[30] A home-made PA cell composed of a duralumin body, a calcium fluoride (CaF_2) window and two valves for gas exchange was used. An FTIR spectrometer (Nicolet, iS10) was used as interference IR sources. The PA signal acquired by a digital MEMS microphone was Fourier-transformed with the Happ-Genzel window function. The PA spectra were obtained by normalizing with

carbon black powder as a reference. Ultraviolet (UV) irradiation was performed through a window on the top of the cell using a light-emitting diode (Nichia NCSU033B, ca. 365 nm, 8.8 mW cm^{-2}).

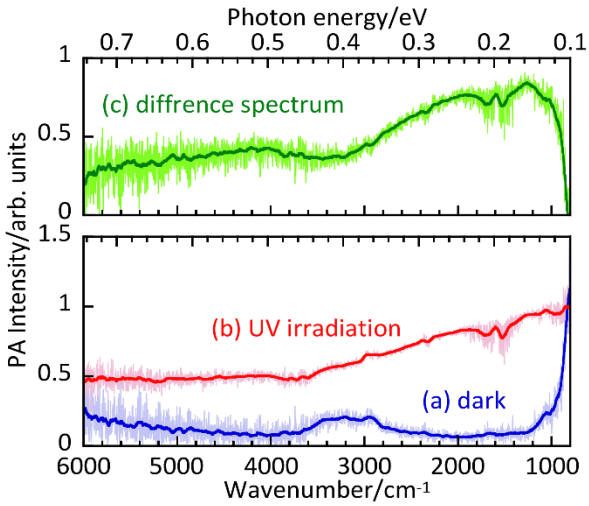

Fig. 1 FTIR-PAS spectra of anatase TiO_2 (AMT-600) with adsorbed ethanol under nitrogen (a) before and (b) after UV irradiation and (c) difference spectrum between (a) and (b). Blue, red and green lines are smoothed spectra by 33 point moving average of original data (pale blue, pink and yellow green lines).

Fig. 1a shows FTIR-PAS spectrum of commercially available anatase TiO_2 (TAYCA Co., AMT-600) with adsorbed ethanol under nitrogen before UV irradiation. Ethanol was used as a hole scavenger to promote electron accumulation in TiO_2. However, unnecessary ethanol was removed because FTIR peaks attributed to an excess amount of ethanol overlaps in the spectrum of TiO_2 and observation of the spectral change is disturbed. As a result, characteristic peaks attributed to organic compounds were not seen clearly and a trace amount of ethanol was adsorbed on the TiO_2. A broad peak around 3200 cm^{-1} is attributed to adsorbed H_2O because a low wavenumber shift of this peak was observed by exposure of TiO_2 to D_2O vapour. The increase in PA intensity in the region of < 1000 cm^{-1} is probably due

to absorption of TiO_2 lattice vibrations.[22,31,32] Another possibility is experimental error due to transmittance loss (< 1000 cm^{-1}) of the CaF_2 window of the PA cell. Repeated measurements before UV irradiation did not cause any notable change in the spectra.

Under UV irradiation, an upward shift of PA intensity without characteristic peaks was observed. This upward shift increased with irradiation time and then it showed a saturation tendency by 30 min of UV irradiation. Fig. 1b shows saturated FTIR-PAS spectrum of anatase TiO_2 (AMT-600) with adsorbed ethanol under nitrogen after UV irradiation. The upward shift depends on the wavenumber and it decreased with an increase of wavenumber, being in agreement with reported results of FTIR studies.[12–23] Difference spectrum between Fig. 1a and b show a peak at 1263 cm^{-1}, corresponding to 0.16 eV of photon energy (Fig. 1c). In order to confirm reproducibility of the results, same experiment was carried out again. The obtained spectra almost coincided with each other (Fig. S2), and correlation coefficients for FTIR-PAS spectra before and after UV irradiation, and difference spectrum were 0.82, 0.96 and 0.912 respectively, indicating that experimental error is negligible small.

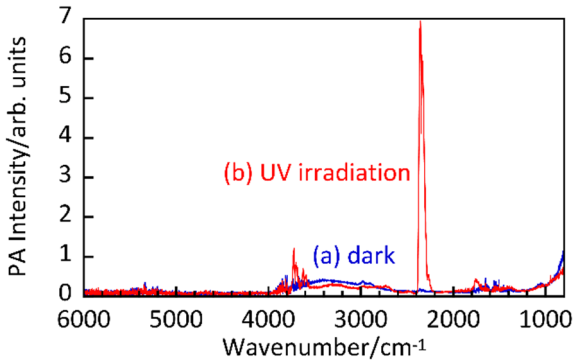

Fig. 2 FTRI-PAS spectra of anatase TiO_2 (AMT-600) with adsorbed ethanol under oxygen (a) before and (b) after UV irradiation.

Fig. 2 shows FTIR-PAS spectra of anatase TiO_2 (AMT-600) with adsorbed ethanol under oxygen before UV irradiation. Before UV irradiation, the spectrum under oxygen were the

same as those under nitrogen. However, they were completely different after UV irradiation. PA spectrum under oxygen show no upward shift, and intense characteristic peaks in the range of 2300–2380 cm^{-1} attributed to gaseous carbon dioxide were observed, while a small peak around 1750 cm^{-1} attributed to aldehyde was seen. Moreover, a noisy peak in the range of 3500–3800 cm^{-1} due to photocatalytic generation of water vapour was observed. These gaseous species are thought to be evolved by photocatalytic oxidation of ethanol over TiO_2. A similar control experiment was carried out under nitrogen in the absence of adsorbed ethanol, and an upward shift was not observed. These results obviously show that both the presence of ethanol as an electron donor and the absence of oxygen as an electron acceptor is necessary for the appearance of an upward shift.

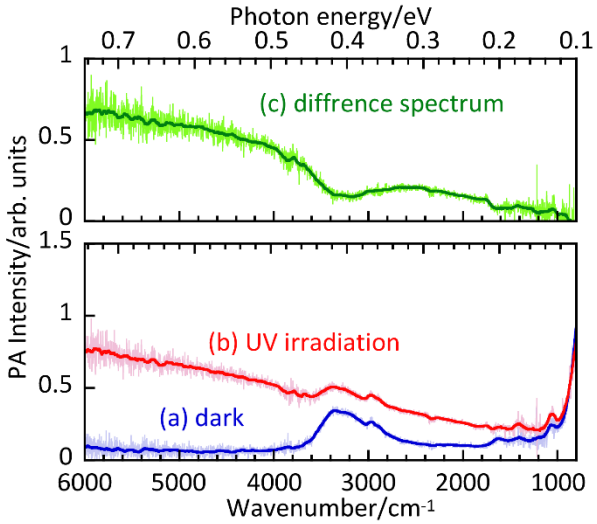

Fig. 3 FTIR-PAS spectra of rutile TiO_2 (MT-150A) with adsorbed ethanol under nitrogen (a) before and (b) after UV irradiation and (c) difference spectrum between (a) and (b). Blue, red and green lines are smoothed spectra by 33 point moving average of original data (pale blue, pink and yellow green lines).

In order to discuss the dependence of crystal structures, the same experiment was carried out for rutile and brookite samples. Both rutile and brookite samples showed spectra similar

to those of anatase before UV irradiation, but the spectral shape under UV irradiation strongly depends on the crystal structure. Fig. 3 shows FTIR-PAS spectra of commercially available rutile TiO_2 (TAYCA Co., MT-150A) with adsorbed ethanol under nitrogen before and after UV irradiation. The rutile sample also showed an upward shift, but it increased with an increase in the wavenumber. In contrast, previous FTIR studies showed that rutile spectra were similar to those of anatase and that the upward shift decreased with an increase in the wavenumber.[16–27] The spectral shape under UV irradiation in the present study resembled that in a transient absorption study.[33] Although peaks in difference spectrum between Fig. 3a and b were not observed due to the limitation of longer wavenumber (Fig. 3c), rutile possesses deeper-energy trapping sites compared to those of anatase.

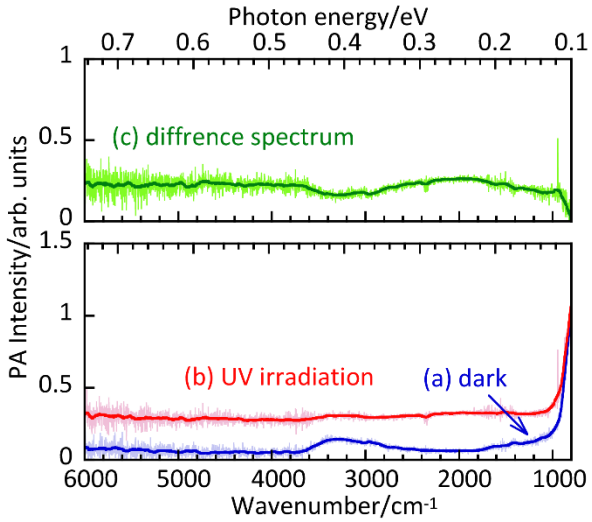

Fig. 4 FTIR-PAS spectra of brookite TiO_2 with adsorbed ethanol under nitrogen (a) before and (b) after UV irradiation and (c) difference spectrum between (a) and (b). Blue, red and green lines are smoothed spectra by 33 point moving average of original data (pale blue, pink and yellow green lines).

Fig. 4 shows FTIR-PAS spectra of commercially available brookite TiO_2 (Kojundo Chemical Laboratory Co.) with adsorbed ethanol under nitrogen before and after UV irradiation. The spectral shape of brookite under UV irradiation was also different from that of anatase or

rutile, and the upward shift was almost constant regardless of the wavenumber. Thus, difference spectrum showed no obvious peak in the region (Fig. 4c). In the present study, the energy level of Ti^{3+} in brookite was not identified, but spectral change of brookite due to electron accumulation was observed for the first time by FTIR measurement.

Other samples with an anatase or rutile crystal structure were also measured (Fig. S3 and S4), and similar spectral change by UV irradiation was observed. It should be noted that the spectrum shape under UV irradiation depends also on sample properties, such as specific surface area, but it mainly depends on crystal structure. It is known that a feature of electron absorption in the IR region depends on the kind of optical transitions.[22] The conduction band electrons exhibit absorbance that increases exponentially as a function of wavelength, and it is attributed to intra-conduction-band transitions. By contrast, electrons in trapping sites show a broad feature as a result of optical transition from trapping states into the conduction band, and the energy of maximum absorbance corresponds to energy levels of trapping states. Therefore, the results in the present study indicate that the energy level of Ti^{3+} is largely determined by crystal structure.

The results indicate that both the absence of acceptors and presence of donors are necessary for the appearance of an upward shift. Thus, it seems that the upward shift is due to Ti^{3+} generated by electron accumulation. In order to confirm this speculation, the relationship between increased PA intensity by UV irradiation and Ti^{3+} density was investigated. The Ti^{3+} density in a TiO_2 sample was measured by the time course of PAS in UV-visible region.[13] In order to estimate the increased PA intensity, the integral value (S_{IV}) was calculated from the difference spectrum in the wavenumber region of 1000–6000 cm^{-1}. Fig. 5 shows S_{IV} of various samples against Ti^{3+} density. S_{IV} showed a linear relationship against Ti^{3+} density, regardless of the crystal structure. The results suggest that the increase of PA intensity is due to Ti^{3+} generated by electron accumulation. Deviation form a linear relationship implies that weight due to the energy level is not considered in the relationship.

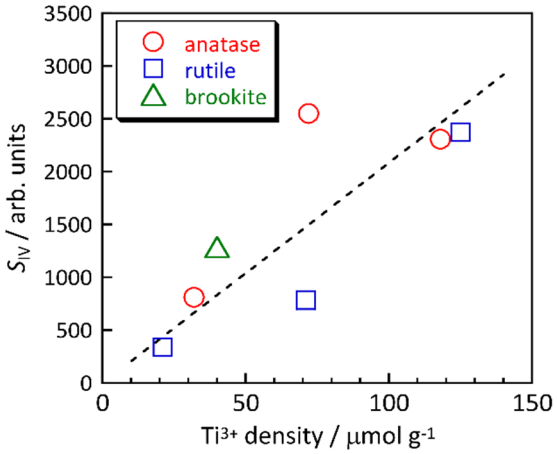

Fig. 5 Relation between S_{IV} and Ti^{3+} density.

In summary, we have shown the application of FTIR-PAS for measurement of the energy level of Ti^{3+}. Regardless of the crystal structure, spectral change due to Ti^{3+} generated by electron accumulation on TiO_2 particles was observed, but the spectral shape was different between crystal structures. These results indicate that rutile has a deeper energy level of electron trapping sites than that of anatase. It is well known that anatase shows higher activity than rutile in a large variety of photocatalytic reaction.[34] Thus, the reason may be explained also by a shallower energy level of electron trapping sites in anatase thought it is believed that it is due to more negative conduction band potential of anatase. On the other hand, the energy level in brookite samples cannot be identified. In order to analyse deeper energy levels, extension of the wavenumber using a near-IR source is now in progress. The present study is the first study showing a difference in energy levels of electron trapping sites between crystal structures by utilization of FTIR.

This work was supported by Grant-in-Aid for Scientific Research(C) (JP17K06019) implemented by the Ministry of Education, Culture, Sports, Science and Technology (MEXT).

Notes and references

1 B. Ohtani, *Catalysts*, 2013, **3**, 942−953.

2 M.R. Hoffmann, S.T. Martin, W. Choi and D.W. Bahnemann, *Chem. Rev.*, 1995, **95**, 69−96.

3 A. Fujishima, T.N. Rao and D.A. Tryk, *J. Photochem. Photobiol. C: Photochem. Rev.*, 2000, **1**, 1−21.

4 Y. Paz, *Appl. Catal. B: Environ.*, 2010, **99**, 448–460.

5 J. Schneider, M. Matsuoka, M. Takeuchi, J. Zhang, Y. Horiuchi, M. Anpo, D. W. Bahnemann, *Chem. Rev.*, 2014, **114**, 9919–9986.

6 D. Spasiano, R. Marotta, S. Malato, P. Fernandez-Ibañez, I. D. Somma, *Appl. Catal. B: Environ.*, 2015, **170–171**, 90–123.

7 S. Ikeda, N. Sugiyama, S. Murakami, H. Kominami, Y. Kera, H. Noguchi, K. Uosaki, T. Torimoto and B. Ohtani, *Phys. Chem. Chem. Phys.*, 2003, **5**, 778−783.

8 R. F. Howe and M. Grätzel, *J. Phys. Chem.*, 1985, **89**, 4495−4499.

9 R. F. Howe and M. Grätzel, *J. Phys. Chem.*, 1987, **91**, 3906−3909.

10 J. M. Coronado, A. J. Maria, J. C. Conesa, K. L. Yeung, V. Augugliaro and J. Soria, *Langmuir*, 2001, **17**, 5368−5374.

11 T. Berger, M. Sterrer, O. Diwald, E. Knözinger, D. Panayotov, T. L. Thompson and J. T. Yates, *J. Phys. Chem. B*, 2005, **109**, 6061−6068.

12 T. Yoshihara, R. Katoh, A. Furube, Y. Tamaki, M. Murai, K. Hara, S. Murata, H. Arakawa and M. Tachiya, *J. Phys. Chem. B*, 2004, **108**, 3817−3823.

13 N. Murakami, O. O. P. Mahaney, R. Abe, T. Torimoto and B. Ohtani, *J. Phys. Chem. C*, 2007, **111**, 11927−11935.

14 A. Nitta, M. Takase, M. Takashima, N. Murakami and B. Ohtani, *Chem. Commun.*, 2016, **52**, 12096−12099.

15 M. Kobielusz, K. Pilarczyk, E. Święt̨ek, K. Szaciłowski and W. Macyk, *Catalysis Today*, 2018, **309**, 35–42.

16 S. H. Szczepankiewicz, A. J. Colussi and M. R. Hoffmann, *J. Phys. Chem. B*, 2000, **104**, 9842−9850.

17 S. H. Szczepankiewicz, J. A. Moss and M. R. Hoffmann, *J. Phys. Chem. B*, 2002, **106**, 2922−2927.

18 D. S. Warren and A. J. McQuillan, *J. Phys. Chem. B*, 2004, **108**, 19373−19379.

19 D. A. Panayotov and J. T. Yates, Jr., *J. Phys. Chem. C*, 2007, **111**, 2959−2964.

20 D. A. Panayotov and J. T. Yates Jr., *Chem. Phys. Lett.*, 2007, **436**, 204–208.

21 D. M. Savory, D. S. Warren and A. J. McQuillan, *J. Phys. Chem. C*, 2011, **115**, 902–907.

22 D. A. Panayotov, S. P. Burrows and J. R. Morris, *J. Phys. Chem. C*, 2012, **116**, 4535−4544.

23 D. A. Panayotov, S. P. Burrows and J. R. Morris, *J. Phys. Chem. C*, 2012, **116**, 6623−6635.

24 T. Berger, J. A. Anta and V. Morales-Flórez, *J. Phys. Chem. C*, 2012, **116**, 11444−11455.

25 T. Berger and J. A. Anta, *Anal. Chem.*, 2012, **84**, 3053−3057.

26 D. M. Savory and A. J. McQuillan, *J. Phys. Chem. C*, 2013, **117**, 23645−23656.

27 D. M. Savory and A. J. McQuillan, *J. Phys. Chem. C*, 2014, **118**, 13680−13692.

28 A. Rosencwaig and A. Gersho, *J. Appl. Phys.*, 1976, **47**, 64−69.

29 A.C. Tam, *Rev. Mod. Phys.*, 1986, **58**, 381−431.

30 N. Murakami and N. Koga, *Catal. Comm.*, 2016, **83**, 1–4.

31 R. J. Gonzalez, R. Zallen and H. Berger, *Phys. Rev. B: Condens. Matter. Mater. Phys.*, 1997, **55**, 7014−7017.

32 A. L. Emiel, J. M. Hensen and J. P. Hofmann, *J. Phys. Chem. C*, 2017, **121**, 10153−10162.

33 A. Yamakata, J. J. M. Vequizo and H. Matsunaga, *J. Phys. Chem. C*, 2015, **119**, 24538−24545.

34 O. O. P. Mahaney, N. Murakami, R. Abe, B. Ohtani, *Chem. Lett.*, 2009, **38**, 238−239.